

CONSUMABLE ELECTRODE PULSED ARGON-ARC WELDING OF SHEET ALUMINIUM ALLOYS

V.S. MASHIN, M.P. PASHULYA, V.A. SHONIN and I.N. KLOCHKOV
 E.O. Paton Electric Welding Institute, NASU, Kiev, Ukraine

Technological features of consumable electrode pulsed argon-arc butt welding of 1.0–2.8 mm thick sheet aluminium alloys AMts, AMg2, AMg6, 1915T1 and AD33T1 were studied. The effect of welding modes on geometrical parameters of welds, their macrostructure and mechanical properties of welded joints is shown. Recommendations on welding technology are given.

Keywords: consumable electrode welding, sheet aluminium alloys, pulsed arc, welding modes, welded joints, weld geometry, mechanical properties

Two arc welding processes — by consumable and non-consumable electrodes in inert gases — are the most widely used in fabrication of sheet structures from aluminium alloys of low- and medium strength. They allow making joints with comparatively high levels of strength and ductility of welds, and provide the required service properties of welded joints [1].

Consumable electrode welding, unlike tungsten electrode welding, provides a more highly-concentrated application of thermal energy of the arc to the metal being welded, deep penetration of aluminium alloys, high welding speeds, narrow HAZ and lower product deformations. Such a process is irreplaceable in making sheet joints, particularly, tee-joints, in

which the process of nonconsumable electrode welding does not ensure a sound formation of the weld and complete penetration of the tee-section walls, because of instability of filler wire melting and arc erring over two sheets [2].

Disadvantages of the process of consumable electrode welding are «coarse-ripple» formation of weld surface, small radius and larger angle of weld transition to base metal surface, as well as considerable losses of volatile alloying elements from the electrode metal [3]. Pores often form in the welds and fusion zone, which result from a relatively high content of hydrogen in the base and filler metal, electrode metal overheating [4] and slight violation of the technological process of welding. Therefore, in keeping with GOST 14806–80, developed at the start of 1970s and still in force now, the process of consumable electrode

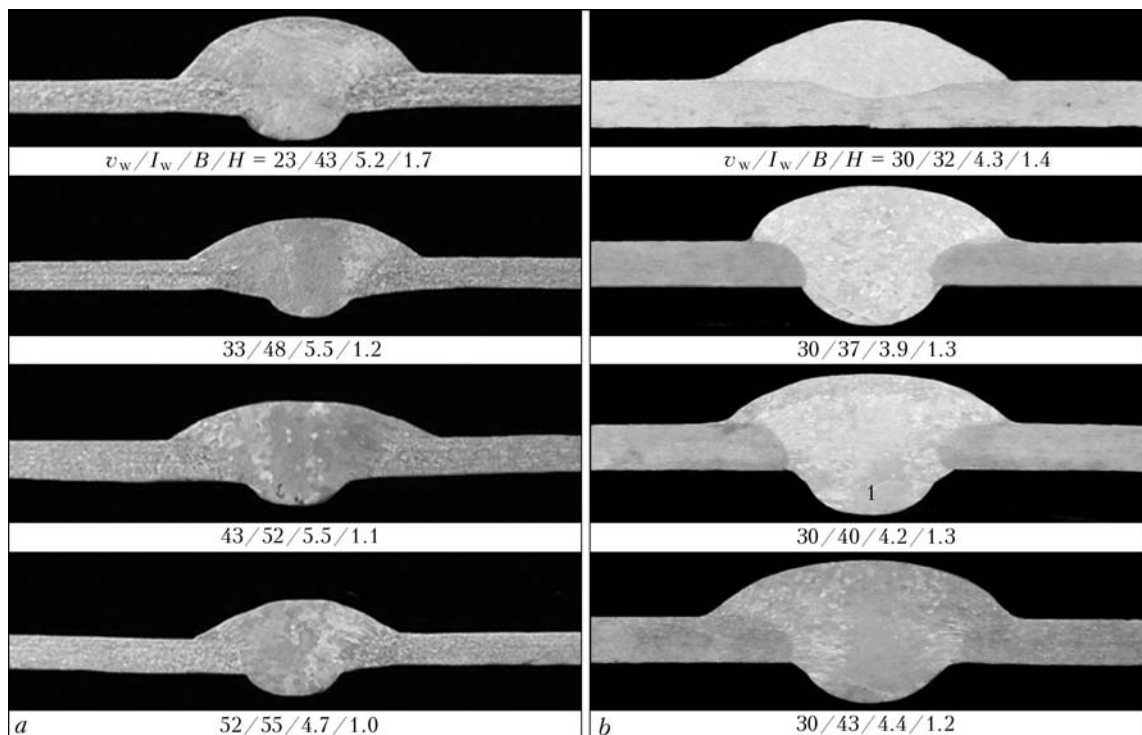


Figure 1. Influence of welding mode on geometry of joints of AMts (a) and AMg2 (b) alloy 1 mm thick. Here and further on the number in the area of weld metal corresponds to the number of test weld with heat input according to Figure 3

welding of aluminium alloys can be applied only for not less than 3 mm thick metal for butt and tee joints and not less than 4 mm metal for fillet and overlap joints.

Consumable electrode pulsed-arc welding, compared to DC welding, allows stabilization of the process of electrode metal drop transfer, improvement of weld formation, reduction of the loss (evaporation) of readily boiling alloying elements from the electrode wire and improvement of mechanical properties of welded joints [5, 6].

Welding machines, including pulsed power sources with synergic control of the process of transfer of electrode metal drops to maintain the synchronous process of «one pulse—one drop» [7] and push-pull type feed mechanisms for welding wires of 0.8–1.6 mm diameter, have been recently manufactured in Europe, USA and Japan. The most efficient of such units are systems of the type of TransPulseSynergic (TPS), which are designed for automated and robotic lines

for manufacturing products for various purposes. Application of this equipment for nonconsumable electrode pulsed-arc welding allows widening the ranges of welded metal thicknesses towards their lowering.

The purpose of these investigations is production of sound joints from sheet aluminium alloys of different aluminium systems up to 3 mm thick when using consumable electrode pulsed argon-arc (MIG) process.

Experimental procedure. Procedure optimization was based on the known principles of the need to reduce thermal impact of the fusion welding process on heat-hardenable aluminium alloys by application of high energy density heat sources. This is achieved, for instance, in laser welding [8], or in hybrid laser-arc consumable electrode welding [9] when helium or helium-argon mixtures ($\text{He} \geq 70\%$) are used as shielding gas [10, 11]. Therefore, at pulsed MIG welding of sheet aluminium alloys relatively high welding currents and increased welding speeds were used as efficient means of welding heat input lowering. In order

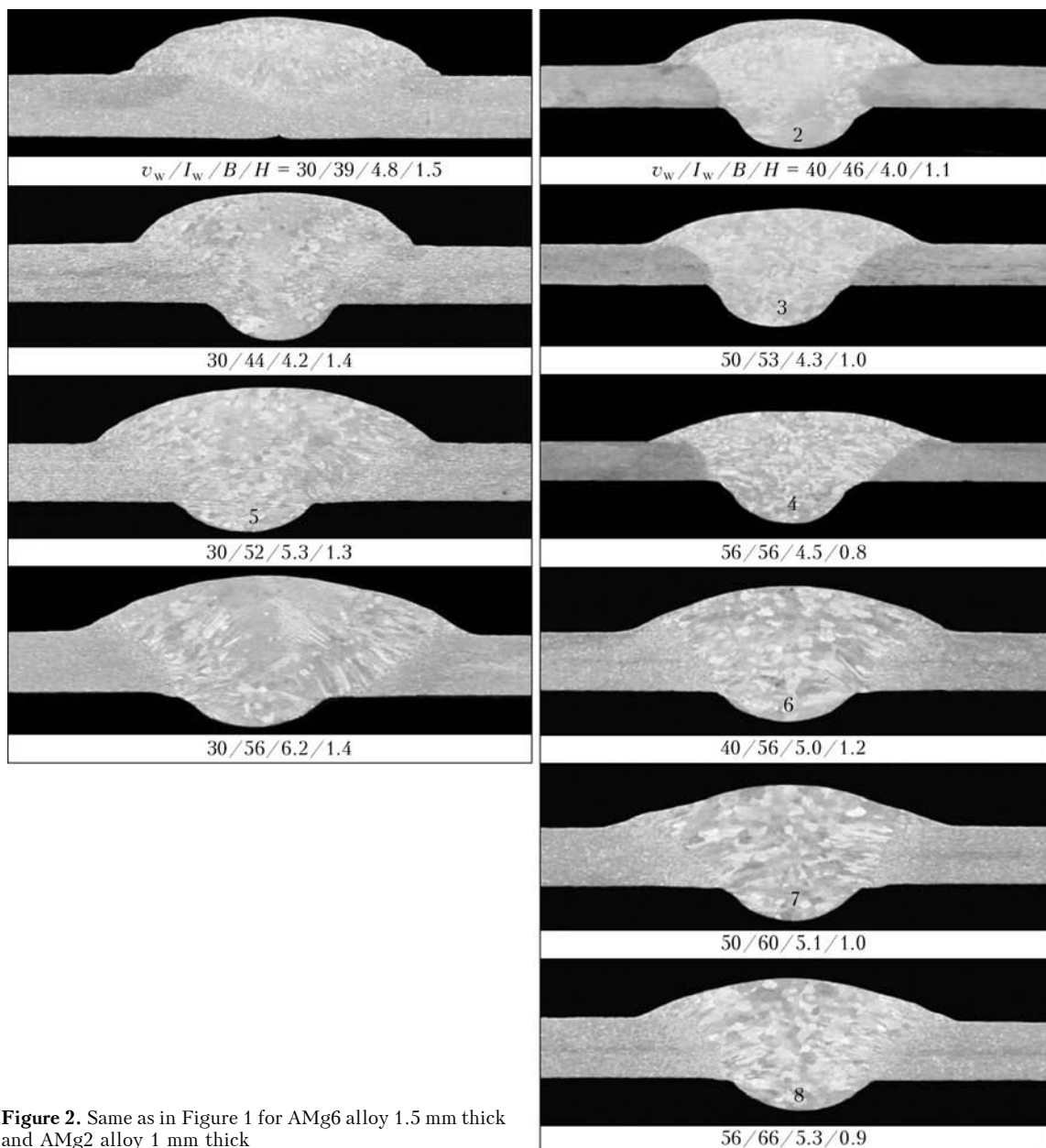


Figure 2. Same as in Figure 1 for AMg6 alloy 1.5 mm thick and AMg2 alloy 1 mm thick



Average values of mechanical properties of welded joints (numerator) made by pulsed MIG welding and base metal (denominator) (in all the tested samples metal rolling direction coincides with weld axis)

Alloy grade	δ , mm	σ_t , MPa	$\sigma_{0.2}$, MPa	$\sigma_{0.01}$, MPa	δ_5 , %	$\sigma_t^{w.j}/\sigma_t^{BM}$	$\sigma_{0.2}^{w.j}/\sigma_{0.2}^{BM}$	Fracture zone
AMg2	1.0	180	82	79	12.3	0.94	1.0	HAZ, BM
AMg2*	1.0	$\frac{177}{192}$	$\frac{80}{82}$	$\frac{78}{80}$	$\frac{12.4}{22}$	0.92	0.98	Same
AMg6	1.5	352	182	146	15	0.96	0.93	FZ and HAZ
AMg6*	1.5	$\frac{312}{365}$	$\frac{171}{196}$	$\frac{139}{148}$	$\frac{12}{20}$	0.85	0.87	Weld
AMg6	1.8	348	166	111	17	0.97	0.86	FZ and HAZ
AMg6*	1.8	$\frac{319}{357}$	$\frac{158}{192}$	$\frac{97}{151}$	$\frac{14}{20}$	0.89	0.82	Weld
AD33T1	2.8	218	126	81	8.8	0.69	0.44	HAZ
AD33*	2.8	$\frac{216}{314}$	$\frac{124}{277}$	$\frac{79}{151}$	$\frac{8.7}{14.9}$	0.68	0.45	Same
1915T1	2.8	346	216	185	9.2	0.82	0.72	BM
1915T1*	2.8	$\frac{297}{426}$	$\frac{173}{297}$	$\frac{155}{205}$	$\frac{5.7}{19}$	0.70	0.58	Weld

*Weld convexities are removed.

to produce sound joints the following principle was applied: the higher the welding current (higher arc voltage and welding speed, respectively), the smaller the weld width and their reinforcement height (at unchanged depth of metal penetration) and, as a consequence, lower residual deformations of the joints.

Aluminium alloys AMts 1 mm thick, AMg2 1 mm thick, AMg6 1.5 and 1.8 mm thick, AD33T1 and 1915T1 2.8 mm thick and SvAMg6 welding wire (GOST 7871-75) of 1.2 mm diameter were used in investigations. Highest grade argon was used as shielding gas. Automatic pulsed MIG welding of butt joints was performed in Fronius TPS-450 welding system. Before welding the metal surface was scraped. Angle of welding torch inclination was 10-15°, distance from torch nozzle to metal being welded was 8-12 mm, argon flow rate being 20 l/min.

Welding of butt joints was performed on removable backing from stainless steel with grooves of 2 mm width and 0.8 mm depth for 1-2 mm alloys, and grooves of 3.8 mm width and 1 mm depth for 2.8 mm alloys. Geometrical parameters of welds – width B and height H of face reinforcement – were determined on transverse macrosections. Values of heat input of pulsed MIG process were calculated by the following formula: $q_{h,i} = K_{ef} I_w U_a / v_w$, kJ/cm, where K_{ef} is the effective arc efficiency (0.72 for argon). Mechanical properties of base metal and welded joints were determined on standard samples to GOST 6996-66.

Figures 1 and 2 give the microstructures of joints of AMts, AMg2 and AMg6 alloys, depending on welding mode. It is determined that the optimum weld width and their smooth transition to base metal are observed at $I_w \geq 55$ A and $v_w \geq 50$ m/h ($q_{h,i} \leq 0.5$ kJ/cm), at v_w of 30 m/h optimum formation of reinforcement is observed at $I_w \leq 40$ A. It should be noted that such a speed ($v_w \leq 30$ m/h) is the most acceptable at semi-automatic process, when the welder still can reliably maintain the welding torch extension and its uniform displacement.

Calculations showed that at maintaining of the same depth of penetration of 1-3 mm thick metal, increase of welding speed by 3 times (for instance from 20 to 60 m/h) requires increasing the welding current by just 1.7 times and increasing the arc voltage only by 1.15 times, leading to 1.6 times lowering of the welding process heat input (Figure 3). This is, most probably, accounted for by the fact that aluminium alloy penetration depth h is proportionately dependent on arc pressure P , which, in its turn, depends on the square of welding current and is determined by the following equation [12]: $h = f(P) \approx B_0 + B_1 I_w + B_2 I_w^2$, where B_0, B_1, B_2 are the coefficients of regression equation dependent on shielding gas composition, diameter and grade of electrode wire, etc.

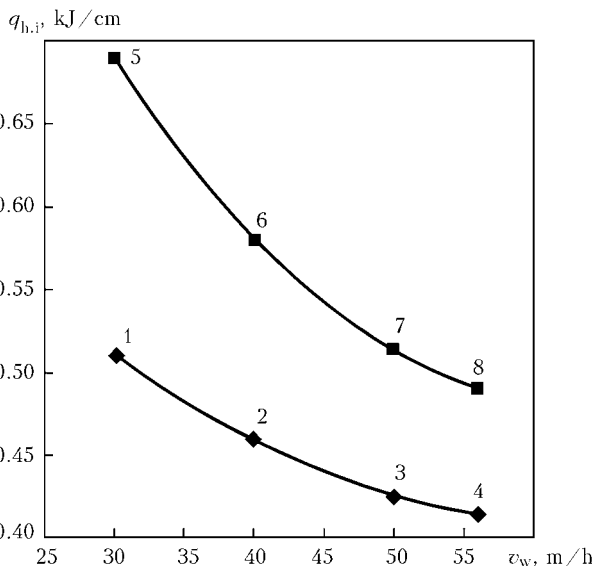


Figure 3. Influence of welding speed on average value of heat input of pulsed MIG welding of AMg2 alloy 1 mm thick (points 1-4) and AMg6 alloy 1.5 mm thick (5-8)

Analysis of the data, given in Figures 1–3, leads to the conclusion that automatic pulsed MIG welding of aluminium alloys 1–2 mm thick should be performed at $I_w \geq 55$ A and $v_w \geq 50$ m/h ($q_{h,i} \leq 0.5$ kJ/cm). This is true for welding technologies without application of systems of following the welding torch displacement over the butt joint edges. In the case the above-mentioned following systems are used, welding speed can be increased considerably.

Figure 4 shows the dimensions of weld reinforcement and macrostructure of joints of 1915T1 alloy, depending on welding modes. It is established that welds of joints made in optimum welding modes ($v_w = 40$ – 50 m/h) have no pores of more than 0.1 mm diameter.

Investigations showed that the geometrical dimensions of welds made by pulsed MIG welding do not exceed the respective values, which are specified by state standards (GOST 14806–80) and industry standards on welded aluminium joints in manual and automatic tungsten-electrode welding.

Results of investigations of mechanical properties of welded joint samples are given in the Table and are indicative of the fact that for non-heat-hardenable alloys of Al–Mg–Mn type the conditional tensile strength of joints (with two-sided weld reinforcement) decreases compared to base metal by not more than 6 %, and proof stress – by not more than 14 %. The greatest lowering of σ_t and $\sigma_{0.2}$, compared to base metal, is observed for joints of heat-hardenable alloys: for AD33T1 alloy – by 32 and 55 %, and for 1915T1 alloy – by 16 and 28 %, respectively. A feature of fracture of welded joints with weld reinforcements consists in that all of them fail beyond the weld metal. With removed reinforcement, joints of AMg2, AMg6 and 1915T1 alloys fails through the weld metal, and lowering of mechanical properties compared to base metal is respectively equal to: for joints of AMg6 alloy σ_t – up to 15 %, $\sigma_{0.2}$ – up to 16 %, for joints of 1915T1 alloy σ_t – up to 16 %, and $\sigma_{0.2}$ – up to 28 %. For joints of AD33 alloy presence or absence of weld reinforcement practically does not affect the values of conditional tensile strength or proof strength, as the joints fail across the HAZ metal.

CONCLUSIONS

1. Modern pulsed power sources with synergic control of pulsed MIG process allow widening the ranges of welded metal thicknesses towards their lower values. Optimization of welding modes, providing stabilization of uniform formation of the weld root, improves the quality of joints of sheet aluminium alloys.

2. Pulsed MIG welding in argon can be used to produce joints of aluminium alloys 1.0–2.8 mm thick with a sufficiently good quality of weld formation and their high tightness. Geometrical dimensions of the deposited metal do not exceed the respective values of parameters of welds made by manual or automatic tungsten electrode welding.

3. In order to lower the heat input of pulsed MIG process and to produce sound joints from sheet aluminium alloys, it is necessary to apply relatively high welding currents and increased welding speeds.

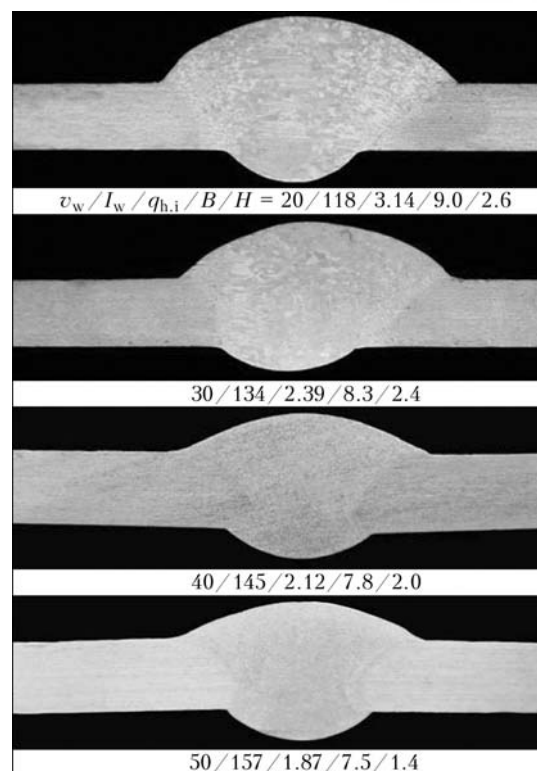


Figure 4. Influence of welding speed, welding current and welding heat input on geometry of welded joints of 1915T1 alloy

4. Results of investigation of the process of pulsed MIG welding of sheet alloys can be used to modify the current state and industry standards for welded joints of aluminium alloys and will promote further wide application of the technology of high-speed consumable electrode welding of sheet products from high-strength aluminium alloys.

- Ishchenko, A.Ya., Labur, T.M., Bernadsky, V.N. et al. (2006) *Aluminium and its alloys in current structures*. Kiev: Ekotekhnologiya.
- Mashin, V.S., Poklyatsky, A.G., Fedorchuk, V.E. (2005) Mechanical properties of aluminium alloy joints in consumable and nonconsumable electrode arc welding. *The Paton Welding J.*, **9**, 39–45.
- Levchenko, O.G., Mashin, V.S. (2003) Sanitary-hygienic characteristic of the process of consumable electrode inert-gas welding of AMg6 aluminium alloy. *Ibid.*, **1**, 46–48.
- Ishchenko, A.Ya., Mashin, V.S., Dovbishchenko, I.V. et al. (1994) Mean temperature of electrode drop metal in inert-gas welding of aluminium alloys. *Avtomatich. Svarka*, **1**, 48–49.
- Mashin, V.S., Pavshuk, V.M., Dovbichchenko, I.V. et al. (1991) Influence of conditions of pulsed arc welding of aluminium AD0 on shape and porosity of welds. *Ibid.*, **4**, 57–60.
- Zhernosekov, A.M., Andreev, V.V. (2007) Pulsed metal-arc welding (Review). *The Paton Welding J.*, **10**, 40–43.
- Voropaj, N.M., Ilyushenko, V.M., Lankin, Yu.N. (1999) Peculiarities of pulsed arc welding with synergic control of welding parameters. *Avtomatich. Svarka*, **6**, 26–31.
- Drits, A.M., Ovchinnikov, V.V. (2009) Peculiarities of laser welding of aluminium-lithium alloys 1420 and 1460. *Tsvetn. Metally*, **9**, 59–63.
- Shelyagin, V.D., Khaskin, V.Yu., Mashin, V.S. et al. (2009) Features of laser-MIG welding of high-strength aluminium alloys. *The Paton Welding J.*, **12**, 21–27.
- Dovbishchenko, I.V., Ishchenko, A.Ya., Mashin, V.S. (1997) Application of helium in consumable electrode welding of aluminium alloys. *Avtomatich. Svarka*, **2**, 14–19.
- Ishchenko, A.Ya., Mashin, V.S., Budnik, V.P. (1995) About porosity of welds in consumable electrode inert-gas welding of aluminium alloys. *Ibid.*, **1**, 16–18.
- Ishchenko, A.Ya., Mashin, V.S., Dovbishchenko, I.V. et al. (1994) Mean temperature of pool metal in inert-gas arc welding of aluminium alloys. *Ibid.*, **11**, 15–19.